HHS Public Access

Author manuscript

Obesity (Silver Spring). Author manuscript; available in PMC 2017 May 28.

Published in final edited form as:

Obesity (Silver Spring). 2017 January ; 25(1): 132–140. doi:10.1002/oby.21692.

Lipidomic profiling of high-fat diet-induced obesity in mice: importance of cytochrome P450-derived fatty acid epoxides

Weicang Wang[1,*], **Jun Yang**[2,*], **Weipeng Qi**[1], **Haixia Yang**[1], **Chang Wang**[2], **Bowen Tan**[2], **Bruce D. Hammock**[2], **Yeonhwa Park**[1], **Daeyoung Kim**[3], and **Guodong Zhang**[1,†]

[1]Department of Food Science, University of Massachusetts, Amherst, MA, 01003

[2]Department of Entomology and Comprehensive Cancer Center, University of California, Davis, CA, 95616

[3]Department of Mathematics and Statistics, University of Massachusetts, Amherst, MA, 01003

Abstract

OBJECTIVE—Enzymatic metabolism of polyunsaturated fatty acids (PUFAs) leads to formation of bioactive lipid metabolites (LMs). Previous studies have shown that obesity leads to deregulation of LMs in adipose tissues. However, most previous studies have focused on single or limited number of LMs, few systematical analyses have been carried out.

METHODS—We used a LC-MS/MS-based lipidomics approach, which can analyze >100 LMs produced by cyclooxygenase (COX), lipoxygenase (LOX), and cytochrome P450 (CYP) enzymes, to analyze profile of LMs in high-fat diet-induced obesity in mice.

RESULTS—LC-MS/MS showed that dietary feeding of high-fat diet significantly modulated profiles of LMs in adipose tissues. Among the three major PUFA metabolizing pathways (COX, LOX, and CYP), CYP-derived fatty acid epoxides were the most dramatically altered LMs. Almost all types of fatty acid epoxides were reduced by 70–90% in adipose tissues of high-fat diet-fed mice. Consistent with the reduced levels of fatty acid epoxides, the gene expressions of several CYP epoxygenases, including *Cyp2j5, Cyp2j6*, and *Cyp2c44*, were significantly reduced in adipose tissues of high-fat diet-fed mice.

CONCLUSIONS—Our results showed that CYP-derived fatty acid epoxides are the most responsive LMs in high-fat diet-induced obesity, suggesting that these LMs could play critical roles in obesity.

Keywords

Obesity; eicosanoids; lipid metabolites; lipidomics; cyclooxygenase; lipoxygenase; cytochrome P450

†To whom correspondence should be addressed: Guodong Zhang, Department of Food Science, University of Massachusetts, Amherst, MA, USA. guodongzhang@umass.edu, Tel: 413-4541014, Fax: 413-5451262.

*W.W. and J.Y. contributed equally to this work.

CONFLICT OF INTEREST

The authors declare no conflict of interest.

INTRODUCTION

Obesity is a major health concern in the US: more than one-third of US adults (34.9% or 78.6 million) are obese (1). Obese individuals have significantly increased risks of developing many diseases, including cardiovascular diseases, hypertension, type II diabetes, and certain types of cancer (2). The annual medical care cost to treat obesity and obesity-assocaited diseases is estimated to be around $190 billion in the US (3). Therefore, it is of critical importance to better understand the mechanism by which obesity increases the risks of various human diseases, which could facilitate the development of effective therapeutic strategies.

The enzymatic metabolism of polyunsaturated fatty acids (PUFAs), such as arachidonic acid (ARA, 20:4ω-6), leads to formation of bioactive lipid metabolites (LMs), which are important lipid signaling molecules involved in regulation of many fundamental physiological and pathological processes (4, 5, 6) (see a simplified scheme in Fig. S1a, the abbreviations of LMs are in Table S1). There are three major pathways involved in enzymatic metabolism of PUFAs: cyclooxygenase (COX-1 and COX-2), lipoxygenase (5-LOX, and 12/15-LOX), and cytochrome P450 (CYP). The COX pathway leads to formation of prostaglandins, which are important mediators to induce inflammation and pain; and COX-2 is the therapeutic target of many anti-inflammatory drugs on the market (4). The LOX pathway produces leukotrienes and hydroxyl fatty acids, which are predominately pro-inflammatory and play critical roles in inflammatory diseases such as asthma (4). The CYP pathway converts PUFAs to fatty acid epoxides, which have a variety of beneficial effects such as anti-inflammatory, cardio-protective, vasodilative, and analgesic actions (5, 6). Besides ARA, other PUFAs, including linoleic acid (LA, 18:2ω-6), α-linolenic acid (α-LA, 18:3ω-3), γ-linolenic acid (γ-LA, 18:3ω-6), dihomo-γ-linolenic acid (DGLA, 20:3ω-6), eicosapentaenoic acid (EPA, 20:5ω-3), and docosahexaenoic acid (DHA, 22:6ω-3), are also efficient alternative substrates of these enzymes and are converted to the corresponding LMs with unique biological activities (6, 7, 8) (Fig. S1b–f). Together, this leads to formation of a large array of LMs with diverse chemical structures, many of which have potent biological activities.

Previous research has shown that LMs play critical roles in pathology of obesity. In obese Zucker rats, there is attenuated production of prostacyclin (PGI_2), which is a LM produced by COX enzymes with potent anti-inflammatory and vasodilative effects (9). Reduced levels of this beneficial LM could contribute to increased adipose inflammation and impaired adipose tissue blood flow (ATBF) in obesity. Dietary feeding of high-fat diet (HFD) increased tissue levels of LOX-derived leukotriene B_4 (LTB_4); and inhibition of LTB_4 receptor protected mice from HFD-induced insulin resistance and hepatic steatosis (10), suggesting that LOX pathway contributes to increased risks of obesity-associated diseases. Dietary feeding of HFD also reduced levels of CYP-derived epoxyeicosatrienoic acids (EETs), which have potent anti-inflammatory, vasodilative, and cardio-protective effects (11, 12, 13). Pharmacological inhibition or transgenic deletion of soluble epoxide hydrolase (sEH, the dominant enzyme in degrading EETs) have been shown to protect mice from

various adverse effects induced by obesity (14, 15, 16, 17, 18, 19, 20, 21). Together, these results support that LMs play critical roles in regulating the pathology of obesity.

Most previous studies of LMs in obesity have only studied single or limited number of LMs (9, 10, 14, 15, 16, 17, 18, 19, 20, 21). However, the enzymatic metabolism of PUFAs produces hundreds of LMs, which could have different or even opposite biological activities, it would be difficult to understand the biological processes by only studying single or limited number of LMs (22). Therefore, it is important to conduct comprehensive profiling of a variety of LMs in tissues, which could help us to better understand their roles in pathology of obesity, in order to develop novel biomarkers or therapeutic targets for obesity and obesity-associated diseases. To this end, here we used a LC-MS/MS-based lipidomics approach, which can simultaneously measure the concentrations of > 100 LMs produced by COX (COX-1, COX-2), LOX (5-LOX, 12/15-LOX) and CYP enzymes from ARA, LA, α-LA, DGLA, EPA, and DHA (23, 24) (see Table S1), to systematically analyze how lipid signaling is deregulated in obesity.

MATERIALS AND METHODS

Obesity experiment

The animal experiment was conducted in accordance with the protocols approved by the Institutional Animal Care and Use Committee of UMass-Amherst. C57BL/6 male mice (6-week age) were maintained on a high-fat diet (60% kcal% fat, purchased from Research Diet Inc., catalog number D12492) and a control diet (10 kcal% fat, D12450J from Research Diet Inc.) for 8 weeks. Diet information can be found at http://www.researchdiets.com/opensourcediets/stock-diets/dio-series-diets.

LC-MS/MS-based lipidomics analysis

To extract lipid metabolites from adipose tissues, ~100 mg tissues were mixed with an antioxidant solution (0.2 mg/mL butylated hydroxytoluene and 0.2 mg/mL triphenylphosphine in methanol), 10 μL of deuterated internal standards (500 nM of d_4-6-keto PGF1a, d_4-TXB_2, d_4-PGE_2, d_4-LTB_4, d_{11}-14,15-DHET, d_4-9-HODE, d_8-5-HETE, d_{11}-11,12-EET), and 400 μL extract solution (0.1% acetic acid with 0.2 mg/mL butylated hydroxytoluene in methanol), and then homogenized; the resulting homogenates were kept in −80 °C overnight. After centrifugation of the homogenates, the pellets were washed with methanol (containing 0.1% butylated hydroxytoluene and 0.1% acetic acid) and then combined with the supernatant. The lipid metabolites in the combined solutions were loaded onto pre-washed Waters® Oasis solid phase extraction (SPE) cartridges, washed with 95:5 v/v water/methanol with 0.1% acetic acid, the analytes were eluted with methanol and ethyl acetate, dried using a centrifugal vacuum evaporator, then reconstituted in methanol for LC-MS/MS analysis. The LC-MS/MS analysis was carried out on an Agilent 1200SL HPLC system (Agilent, Santa Clara, CA) coupled to a 4000 QTRAP MS/MS (AB Sciex, Foster City, CA) as described in our previous report (24). The lipid mediators whose levels were above the detection limit of LC-MS/MS were reported.

Real-time PCR (RT-PCR) analysis

Total RNA was isolated from gonadal adipose tissues using TRIzol Reagent (Life technologies, Carlsbad, CA) according to manufacturer's instruction. Conversion of up to 2 μg of total RNA to single stranded cDNA was preformed using High-Capacity cDNA Reverse Transcription Kit (Life technologies, Carlsbad, CA) according to manufacturer's instruction. Quantitative RT-PCR was conducted using Maxima SYBR Green/ROX qPCR Master Mix (Thermo Fisher Scientific, Agawam, MA) on a DNA Engine Opticon® 2 System (Bio-Rad Laboratories, Hercules, CA) with specific mouse primers. The primers used in this research were: *Cyp2j5* (sense) 5'-TCTGGGAAGCACTCCATCTCA-3' and (antisense) 5'-CCCTGGTGGGTAGTTTTTGG-3', *Cyp2j6* (sense) 5'-TTAGCCACGATCTGGGCAG-3' and (antisense) 5'-CTGGGGGATAGTTCTTGGGG-3', *Cyp2c44* (sense) 5'-GCTGCCCTATACAGATGCCG-3' and (antisense) 5'-GTGACGCTAAGAGTTGCCCA-3', *Ephx2* (sense) 5'-GCGTTCGACCTTGACGGAG-3' and (antisense) 5'-TGTAGCTTTCATCCATGAGTGGT-3', *Alox15* (sense) 5'-GGCTCCAACAACGAGGTCTAC-3' and (antisense) 5'-AGGTATTCTGACACATCCACCTT-3', *Alox5* (sense) 5'-ACTACATCTACCTCAGCCTCATT-3' and (antisense) 5'-GGTGACATCGTAGGAGTCCAC-3', *Cox2* (sense) 5'-TTCAACACACTCTATCACTGGC-3' and (antisense) 5'-AGAAGCGTTTGCGGTACTCAT-3', *Pla2* (sense) 5'-TGCCTTTCCTGTAGGCTGTTC-3' and (antisense) 5'-CGCAGGTCTCGTAGCATCTG-3', *Ptges* (sense) 5'-GGATGCGCTGAAACGTGGA-3' and (antisense) 5'-CAGGAATGAGTACACGAAGCC-3', *Ptgis* (sense) 5'-ACAGCATCAAACAATTTGTCGTC-3' and (antisense) 5'-GCATCAGACCGAAGCCATATCT-3', *Pla2g4a* (sense) 5'-CAGCACATTATAGTGGAACACCA-3' and (antisense) 5'-AGTGTCCAGCATATCGCCAAA-3', *Pla2g12a* (sense) 5'-TGCCTTTCCTGTAGGCTGTTC-3' and (antisense) 5'-CGCAGGTCTCGTAGCATCTG-3'. The results of target genes were normalized to *β-actin* gene and expressed to the control group mice using the $2^{-\Delta\Delta Ct}$ method. The primer to analyze *β-actin* is (sense) 5'-GGCTGTATTCCCCTCCATCG-3' and (antisense) 5'-CCAGTTGGTAACAATGCCATGT-3'.

Fatty acid composition analysis

Total lipids from gonadal adipose tissue were extracted as previously described (25), then treated with 3 N methanolic HCl at 55°C for 40 minutes to prepare the fatty acid methyl esters (FAMEs) (26). The resulted FAMEs dissolved in hexane were used for GC-MS analysis, using Shimadzu GC-MS-QP2010 SE (Tokyo, Japan). Oven conditions: initial temperature 50°C; temperature increase: 20°C/min to 200 °C, then increase 2°C/min to 220°C and held for 142.5 minutes. Other conditions: injector temperature 250 °C; detector temperature 250 °C; carrier gas helium, split ratio: 10:1. Column: Supelcowax 10 (fused silica), 100 m × 0.25 mm × 0.25 Pm. The FAMEs were identified by comparing with the standards (Sigma-Aldrich, St. Louis, MO, or Nu-Chek Prep, Elysian, MN) or by their mass spectra, which were further compared to the NIST Mass Spectral library.

Data Analysis

All data are expressed as the mean ± standard error of the mean (SEM). For the comparison between the control group and HFD group, Shapiro-Wilk test was used to verify the normality of data. When data were normally distributed, statistical significance was determined using two-side t-test; otherwise, significance was determined by Mann-Whitney U test. All of these data analysis was performed by using SigmaPlot software (San Jose, CA). The principal component analysis (PCA) was implemented using MetaboAnalyst (http://www.metaboanalyst.ca/). The data were scaled using auto scaling before the analysis. P values less than 0.05 are reported as statistically significant.

RESULTS

CYP-derived LMs in adipose tissues

After 8 weeks of dietary feeding, HFD significantly increased body weight and adipose tissue weight in C57BL/6 mice (Fig. S2). These results are consistent with previous studies of HFD on obesity (27). We used LC-MS/MS-based lipidomics to compare the profiles of LMs in inguinal, gonadal, and interscapular adipose tissues of mice fed on HFD or control diet. Among the three major PUFA metabolizing pathways (COX, LOX, and CYP), CYP-derived fatty acid epoxides are the most dramatically altered LMs in adipose tissues (Fig. 1 and Fig. S3). PCA analysis of the lipidomics data shows the difference between HFD group from control group, and fatty acid epoxides were the most important lipid mediators contributing to the differentiation (Fig. S3). The levels of fatty acid epoxides derived from several PUFAs, including epoxyoctadecenoic acids (EpOMEs) derived from LA, EETs from ARA, epoxydocosapentaenoic acids (EpDPEs) from DHA, and epoxyoctadecadienoic acids (EpODEs) from α-LA, were significantly reduced in different adipose tissues (inguinal, gonadal, and interscapular fats) of HFD-fed mice (Fig. 2a–c). For example, the concentrations of 11,12-EET and 14,15-EET were reduced by respective 88±20% and 89±18% in inguinal adipose tissues ($P \leq 0.001$), and were reduced by respective 88±13% and 89±11% in gonadal fat tissues of HFD-fed mice ($P \leq 0.001$) (Fig. 2a–b). The ratios of fatty acid epoxides to the corresponding diols were also reduced in the tissues of HFD-fed mice (Fig. S4). There is no difference in terms of recovery of deuterated LM standards between control and HFD group (see Fig. S5).

The fatty acid epoxides are further metabolized by soluble epoxide hydrolase (sEH) to generate the corresponding fatty acid diols (10). Consistent with reduced adipose levels of fatty acid epoxides, the levels of fatty acid diols were also significantly reduced (Fig. 2a–c). For example, the levels of 11,12-dihydroxyeicosatrienoic acid (11,12--DHET), which is a sEH metabolite of 11,12-EET, were reduced by 54.5±10.7% (mean ± SEM) in gonadal adipose tissues of HFD-fed mice ($P \leq 0.001$) (Fig. 2b). We need to point out in the adipose tissues, the concentrations of fatty acid epoxides were much higher than those of the corresponding fatty acid diols. For example, the concentration of 11,12-EET was ~73-fold higher than its sEH metabolite 11,12-DHET in gonadal adipose tissues of control mice (Fig. 2b).

We further analyzed whether there is a correlation of adipose tissue weight with adipose concentration of CYP-derived LMs. In gonadal fat tissues, the adipose tissue weight inversely correlated with adipose concentration of fatty acid epoxides such as 11,12-EET and 19,20-EpDPE (Fig. 2d), supporting a critical role of these fatty acid epoxides in obesity.

COX-derived LMs in adipose tissues

The metabolism of PUFAs by COX enzymes lead to formation of prostaglandin H_2 (PGH_2), which was further enzymatically metabolized to generate various prostaglandins (Fig. 3a). Compared with CYP-derived LMs, the profiles of COX-derived LMs showed more complicated patterns. In inguinal adipose tissues, the levels of COX-derived LMs were not changed (Fig. 3b), suggesting that COX pathway is not likely to be involved in the biology of inguinal adipose tissues. In gonadal adipose tissues, the concentrations of PGI_2 (as measured by its stable metabolite 6-keto-PGF_{1a}) and PGE_2 were significantly reduced in HFD-fed mice (Fig. 3c). In interscapular adipose tissues, the concentrations of $PGF_{2\alpha}$ and PGE_2 were significantly reduced in HFD-fed mice ($P < 0.05$, Fig. 3d).

5-LOX-derived LMs in adipose tissues

The metabolism of ARA by 5-LOX leads to formation of 5-hydroperoxyeicosatetraenoic acid (5-HpETE), which is then converted to at least two classes of LMs: (1) 5-hydroxyeicosatetraenoic acid (5-HETE), or similar LMs such as α-LA-derived 9-HOTrE and EPA-derived 5-HEPE, and (2) LTB_4, or similar LMs such as EPA-derived leukotriene B_5 (LTB_5) (Fig. 4a). Dietary feeding of HFD reduced levels of 5-HETE-series LMs (such as 5-HETE, 9-HOTrE, and 5-HEPE), while increased levels of LTB_4 in adipose tissues (Fig. 4b–d). The tissue levels of LTB_4 were significantly increased in inguinal, gonadal, and interscapular adipose tissues of HFD-fed mice (Fig. 4b–d), which is in agreement with recent studies which showed that HFD increased tissue levels of LTB_4 (10).

12/15-LOX-derived LMs in adipose tissues

The metabolism of PUFAs by 12/15-LOX leads to formation of a series of LMs (Fig. 5a). LC-MS/MS showed that many of these LMs were reduced in adipose tissues of HFD-fed mice (Fig. 5b–d). For example, the tissue levels of 15-HETE were significantly reduced in inguinal, gonadal, and interscapular adipose tissues of HFD-fed mice (Fig. 5b–d). 12-HETE, which is among the most abundant LOX-derived LMs in adipose tissues, was reduced by 71.7±6.78% (mean ± SEM) in interscapular adipose tissue of HFD-fed mice (Fig. 5d).

Fatty acid composition and expression of COX, LOX and CYP in adipose tissues

The tissue profiles of LMs are in part mediated by fatty acid composition and expression of PUFA metabolizing enzymes in the tissues (6). To understand the mechanisms by which HFD modulated LMs in adipose tissues, we analyzed fatty acid composition and gene expression of COX, LOX and CYP in adipose tissues. We focused on gonadal adipose tissues, which are the largest adipose tissues, since we have observed significant changes of most LMs in gonadal fat (Fig. 1–5).

For fatty acid composition, as expected, triglycerides were major lipids in the gonadal adipose tissue, with minimum amount of phospholipids (determined by TLC method based

on Ref (28), data not shown), which is consistent to previous studies (29). Therefore, we analyzed fatty acid composition from the total lipid of adipose tissues. GC-MS analysis showed that dietary feeding of HFD did not change the tissue levels of ARA and α-LA, and slightly increased tissue levels of LA (22.50±0.18% in HFD group *vs.* 17.78±0.44% in control group, $P < 0.001$) (Table. S2). These results support that dietary feeding of HFD did not reduce levels of PUFAs in adipose tissues, suggesting that the reduced levels of many LMs in adipose tissues were not due to lack of PUFA substrates.

For gene expressions of PUFA metabolizing enzymes, RT-PCR showed that the expressions of several CYP epoxygenases, such as *Cyp2j5, Cyp2j6*, and *Cyp2c44*, were significantly reduced in the gonadal adipose tissues of HFD-fed mice (Fig. 6a), which is well consistent with the reduced levels of CYP-derived fatty acid epoxides in adipose tissues (see Fig. 2b). The expression of *Ephx2* (encoding sEH) was not changed (Fig. 6a). For COX pathway, the gene expression of *Cox2* was not changed, while the expressions of *Ptges* (encoding microsomal prostaglandin E synthase) and *Ptgis* (encoding PGI_2 synthase) were significantly reduced in HFD-fed mice (Fig. 6b). This is consistent with the LC-MS/MS analysis which showed that only PGE_2 and PGI_2, but not other COX-derived LMs, were reduced in adipose tissues of HFD-fed mice (Fig. 3c). For LOX pathways, the gene expressions of *Alox15* (encoding 12/15-LOX) and *Alox5* (encoding 5-LOX) were not significantly changed (Fig. 6c), suggesting that the effects of HFD on LOX-derived LMs may be though modulations of down-stream enzymes. Finally, we analyzed the expression of *Pla2* (including cytosolic calcium-dependent *Pla2g4a* and secretory *Pla2g12a* (4)), and found little change of this gene (Fig. 6c). Together, these results support that HFD changed tissue profiles of LMs mainly through modulation of the expressions of PUFA metabolizing enzymes in adipose tissues.

DISCUSSION

In this study, we conducted a LC-MS/MS-based lipidomics analysis of HFD-induced obesity in mice. Our central finding is that HFD significantly modulated the profiles of LMs in adipose tissues of mice. Among the three major PUFA metabolizing pathways (COX, LOX and CYP), CYP-derived fatty acid epoxides are the most dramatically changed LMs in adipose tissues of HFD-induced obesity. Almost all types of fatty acid epoxides, including EpOMEs derived from LA, EETs from ARA, EpDPEs from DHA, and EpODEs from α-LA, were reduced by 70–90% in different types of adipose tissues. Based on our GC-MS analysis of fatty acid composition and RT-PCR analysis of PUFA metabolizing enzymes, these changes were most likely caused by reduced expressions of CYP epoxygenases, not because the PUFA substrates were reduced in adipose tissues of HFD-fed mice. The ratios of fatty acid epoxides to the corresponding diols were reduced in the tissues of HFD-fed mice, while the gene expression of *Ephx2* (encoding sEH) was not changed. This may be because the fatty acid diols could be further metabolized, such as by phase II enzymes through conjugations of the hydroxyl groups, leading to removal of fatty acid diols (6). Our results are consistent with previous studies, which showed that EETs are reduced in adipose tissues of HFD-fed mice (11). Many of these fatty acid epoxides have beneficial effects on health. ARA-derived EETs have been shown to have potent anti-inflammatory, vasodilative, anti-hypertensive, cardio-protective, renal-protective, and analgesic actions (30). DHA-derived

EpDPEs have been shown to be the most potent fatty acid epoxides in dilation of blood vessels, with EC_{50} values of 0.5–24 pM for dilation of porcine coronary arterioles (31). Our own study has shown that EDPs have potent anti-angiogenic, anti-cancer and anti-metastatic effects *in vitro* and *in vivo* (32). Therefore, reduced levels of these beneficial LMs, in particular EETs and EDPs, may contribute to the adverse effects of obesity. This is supported by recent studies, which showed that pharmacological inhibition or transgenic deletion of sEH, which is the dominant enzyme in degrading fatty acid epoxides, protected mice form various adverse consequences of obesity, such as endoplasmic reticulum stress, metabolic syndrome, hepatic steatosis, inflammation, and endothelial dysfunction (11, 14, 15, 16, 17, 18, 19, 20, 21). Together, these results strongly support that CYP-derived fatty acid epoxides play important roles in regulating pathology of obesity.

The profiles of COX- and LOX-derived LMs showed more complicated pattern in adipose tissues of HFD-induced obesity. For COX pathway, the relative balance of vasodilative PGI_2 (as measured by its stable metabolite 6-keto-PGF_{1a}) and vasoconstrictive TXA_2 (as measured by its stable metabolite TXB_2) plays critical role in regulating vascular tone and cardiovascular functions (4, 33). Our study showed that dietary feeding of HFD reduced adipose levels of vasodilative PGI_2, while had little effect on vasoconstrictive TXA_2. These results support that PGI_2 pathway, but not TXA_2 pathway, may contribute to some adverse effects of obesity. Our results are consistent with previous studies which showed that biosynthesis of PGI_2, but not TXA_2, was attenuated in obese Zucker rats (9). We also found that the tissue levels of PGE_2 were significantly reduced in obese mice. This is consistent with previous studies of HFD on adipose tissue levels of PGE_2 (34, 35, 36, 37). The biological significance of PGE_2 remains to be determined. On one hand, PGE_2 is a potent vasodilator, reduced level of PGE_2 could contribute to reduced ATBF of obesity (4); on the other hand, PGE_2 is a potent inducer of inflammation (4), reduced level of PGE_2 is not consistent with the enhanced adipose inflammation in obesity. Previous studies have shown that HFD induced a dynamic change of adipose level of PGE_2: in the early stage of HFD feeding (day 4 post HFD feeding), PGE_2 was increased in adipose tissues; while at a later stage (day 14), its concentration was reduced in adipose tissues (35). These results support that there may be a highly time-dependent change of tissue levels of LMs, in order to respond to varied cellular stimulations at different stages of obesity development.

For LOX pathway, only the concentration of 5-LOX-derived LTB_4 was significantly increased in adipose tissues. This is consistent with recent studies which showed that HFD increased tissue levels of LTB_4; in addition, inhibition of LTB_4 receptor protected mice from HFD-induced insulin resistance and hepatic steatosis (10), supporting a critical role of LTB_4 in pathology of obesity. For 12/15-LOX pathway, our results showed that the many 12/15-LOX-derived LMs 12-HETE, 15-HETE, 15(s)-HETrE, and 13-HOTrE) were reduced in adipose tissues of HFD-fed mice. Our results are consistent with previous studies which showed that HFD reduced adipose concentrations of 12-HETE and 15-HETE (37). Some previous studies have shown that 12/15-LOX pathway is activated in obesity (38); and these different results could be because different animal models of obesity are used. Many of the LOX-derived hydroxyl fatty acids and leukotrienes have potent effects to regulate inflammation and vascular tone (4). It remains to determine whether reduced levels of 12/15-LOX-derived LMs contributed to adverse effects of obesity.

In conclusion, our lipidomics analysis showed that HFD significantly modulated the profiles of LMs in adipose tissues of mice. In particular, CYP-derived fatty acid epoxides are the most dramatically altered LMs in HFD-induced obesity, suggesting that these novel LMs could play critical roles in pathology of obesity. This lipidomics study lays the foundation to further investigate the functional roles of LMs in obesity, which could facilitate the development of novel biomarkers or therapeutic targets for obesity and obesity-associated diseases.

Supplementary Material

Refer to Web version on PubMed Central for supplementary material.

Acknowledgments

This work was partially supported by a new faculty start-up fund, Armstrong Fund of Science Award from UMass-Amherst, and USDA NIFA 2016-67017-24423. In addition, the research is supported in part by USDA grant under project number MAS00450 and MAS00492, and NIEHS R01 ES002710 and Superfund Research Program P42 ES04699.

References

1. Ogden CL, Carroll MD, Kit BK, Flegal KM. Prevalence of childhood and adult obesity in the United States, 2011–2012. JAMA. 2014; 311:806–814. [PubMed: 24570244]
2. Must A, Spadano J, Coakley EH, Field AE, Colditz G, Dietz WH. The disease burden associated with overweight and obesity. JAMA. 1999; 282:1523–1529. [PubMed: 10546691]
3. Spieker EA, Pyzocha N. Economic Impact of Obesity. Prim Care. 2016; 43:83–95. viii–ix. [PubMed: 26896202]
4. Funk CD. Prostaglandins and leukotrienes: advances in eicosanoid biology. Science. 2001; 294:1871–1875. [PubMed: 11729303]
5. Zeldin DC. Epoxygenase pathways of arachidonic acid metabolism. J Biol Chem. 2001; 276:36059–36062. [PubMed: 11451964]
6. Zhang G, Kodani S, Hammock BD. Stabilized epoxygenated fatty acids regulate inflammation, pain, angiogenesis and cancer. Prog Lipid Res. 2014; 53:108–123. [PubMed: 24345640]
7. Arnold C, Markovic M, Blossey K, Wallukat G, Fischer R, Dechend R, et al. Arachidonic acid-metabolizing cytochrome P450 enzymes are targets of omega-3 fatty acids. J Biol Chem. 2010; 285:32720–32733. [PubMed: 20732876]
8. Wang W, Zhu J, Lyu F, Panigrahy D, Ferrara KW, Hammock B, et al. Omega-3 Polyunsaturated fatty acids-derived lipid metabolites on angiogenesis, inflammation and cancer. Prostaglandins Other Lipid Mediat. 2014; 113–115C:13–20.
9. Hodnett BL, Dearman JA, Carter CB, Hester RL. Attenuated PGI2 synthesis in obese Zucker rats. Am J Physiol Regul Integr Comp Physiol. 2009; 296:R715–R721. [PubMed: 19118096]
10. Li P, Oh da Y, Bandyopadhyay G, Lagakos WS, Talukdar S, Osborn O, et al. LTB4 promotes insulin resistance in obese mice by acting on macrophages, hepatocytes and myocytes. Nat Med. 2015; 21:239–247. [PubMed: 25706874]
11. Zha W, Edin ML, Vendrov KC, Schuck RN, Lih FB, Jat JL, et al. Functional characterization of cytochrome P450-derived epoxyeicosatrienoic acids in adipogenesis and obesity. J Lipid Res. 2014; 55:2124–2136. [PubMed: 25114171]
12. Zhou Y, Lin S, Chang HH, Du J, Dong Z, Dorrance AM, et al. Gender differences of renal CYP-derived eicosanoid synthesis in rats fed a high-fat diet. Am J Hypertens. 2005; 18:530–537. [PubMed: 15831364]

13. Theken KN, Deng Y, Schuck RN, Oni-Orisan A, Miller TM, Kannon MA, et al. Enalapril reverses high-fat diet-induced alterations in cytochrome P450-mediated eicosanoid metabolism. Am J Physiol Endocrinol Metab. 2012; 302:E500–E509. [PubMed: 22185841]
14. Bettaieb A, Nagata N, AbouBechara D, Chahed S, Morisseau C, Hammock BD, et al. Soluble epoxide hydrolase deficiency or inhibition attenuates diet-induced endoplasmic reticulum stress in liver and adipose tissue. J Biol Chem. 2013; 288:14189–14199. [PubMed: 23576437]
15. do Carmo JM, da Silva AA, Morgan J, Jim Wang YX, Munusamy S, Hall JE. Inhibition of soluble epoxide hydrolase reduces food intake and increases metabolic rate in obese mice. Nutr Metab Cardiovasc Dis. 2012; 22:598–604. [PubMed: 21190818]
16. Imig JD, Walsh KA, Hye Khan MA, Nagasawa T, Cherian-Shaw M, Shaw SM, et al. Soluble epoxide hydrolase inhibition and peroxisome proliferator activated receptor gamma agonist improve vascular function and decrease renal injury in hypertensive obese rats. Exp Biol Med (Maywood). 2012; 237:1402–1412. [PubMed: 23354399]
17. Iyer A, Kauter K, Alam MA, Hwang SH, Morisseau C, Hammock BD, et al. Pharmacological inhibition of soluble epoxide hydrolase ameliorates diet-induced metabolic syndrome in rats. Exp Diabetes Res. 2012; 2012:758614. [PubMed: 22007192]
18. Liu Y, Dang H, Li D, Pang W, Hammock BD, Zhu Y. Inhibition of soluble epoxide hydrolase attenuates high-fat-diet-induced hepatic steatosis by reduced systemic inflammatory status in mice. PLoS One. 2012; 7:e39165. [PubMed: 22720061]
19. Lopez-Vicario C, Alcaraz-Quiles J, Garcia-Alonso V, Rius B, Hwang SH, Titos E, et al. Inhibition of soluble epoxide hydrolase modulates inflammation and autophagy in obese adipose tissue and liver: role for omega-3 epoxides. Proc Natl Acad Sci U S A. 2015; 112:536–541. [PubMed: 25550510]
20. Roche C, Besnier M, Cassel R, Harouki N, Coquerel D, Guerrot D, et al. Soluble epoxide hydrolase inhibition improves coronary endothelial function and prevents the development of cardiac alterations in obese insulin-resistant mice. Am J Physiol Heart Circ Physiol. 2015; 308:H1020–H1029. [PubMed: 25724490]
21. Zhang LN, Vincelette J, Chen D, Gless RD, Anandan SK, Rubanyi GM, et al. Inhibition of soluble epoxide hydrolase attenuates endothelial dysfunction in animal models of diabetes, obesity and hypertension. Eur J Pharmacol. 2011; 654:68–74. [PubMed: 21187082]
22. Astarita G, Kendall AC, Dennis EA, Nicolaou A. Targeted lipidomic strategies for oxygenated metabolites of polyunsaturated fatty acids. Biochim Biophys Acta. 2015; 1851:456–468. [PubMed: 25486530]
23. Yang J, Dong H, Hammock BD. Profiling the regulatory lipids: another systemic way to unveil the biological mystery. Curr Opin Lipidol. 2011; 22:197–203. [PubMed: 21537174]
24. Yang J, Schmelzer K, Georgi K, Hammock BD. Quantitative profiling method for oxylipin metabolome by liquid chromatography electrospray ionization tandem mass spectrometry. Anal Chem. 2009; 81:8085–8093. [PubMed: 19715299]
25. Folch J, Lees M, Sloane-Stanley G. A simple method for the isolation and purification of total lipids from animal tissues. J biol Chem. 1957; 226:497–509. [PubMed: 13428781]
26. Park Y, Albright KJ, Cai ZY, Pariza MW. Comparison of methylation procedures for conjugated linoleic acid and artifact formation by commercial (trimethylsilyl) diazomethane. Journal of Agricultural and Food Chemistry. 2001; 49:1158–1164. [PubMed: 11312828]
27. Hariri N, Thibault L. High-fat diet-induced obesity in animal models. Nutr Res Rev. 2010; 23:270–299. [PubMed: 20977819]
28. Juaneda P, Rocquelin G. Rapid and convenient separation of phospholipids and non phosphorus lipids from rat heart using silica cartridges. Lipids. 1985; 20:40–41. [PubMed: 2982073]
29. Chen W, Zhou H, Liu S, Fhaner CJ, Gross BC, Lydic TA, et al. Altered lipid metabolism in residual white adipose tissues of Bscl2 deficient mice. PloS one. 2013; 8:e82526. [PubMed: 24358199]
30. Morisseau C, Hammock BD. Impact of soluble epoxide hydrolase and epoxyeicosanoids on human health. Annu Rev Pharmacol Toxicol. 2013; 53:37–58. [PubMed: 23020295]
31. Ye D, Zhang D, Oltman C, Dellsperger K, Lee HC, VanRollins M. Cytochrome p-450 epoxygenase metabolites of docosahexaenoate potently dilate coronary arterioles by activating large-

conductance calcium-activated potassium channels. J Pharmacol Exp Ther. 2002; 303:768–776. [PubMed: 12388664]

32. Zhang G, Panigrahy D, Mahakian LM, Yang J, Liu JY, Stephen Lee KS, et al. Epoxy metabolites of docosahexaenoic acid (DHA) inhibit angiogenesis, tumor growth, and metastasis. Proc Natl Acad Sci U S A. 2013; 110:6530–6535. [PubMed: 23553837]
33. Cheng Y, Austin SC, Rocca B, Koller BH, Coffman TM, Grosser T, et al. Role of prostacyclin in the cardiovascular response to thromboxane A2. Science. 2002; 296:539–541. [PubMed: 11964481]
34. Virtue S, Masoodi M, de Weijer BA, van Eijk M, Mok CY, Eiden M, et al. Prostaglandin profiling reveals a role for haematopoietic prostaglandin D synthase in adipose tissue macrophage polarisation in mice and humans. Int J Obes (Lond). 2015; 39:1151–1160. [PubMed: 25801691]
35. Neuhofer A, Zeyda M, Mascher D, Itariu BK, Murano I, Leitner L, et al. Impaired local production of proresolving lipid mediators in obesity and 17-HDHA as a potential treatment for obesity-associated inflammation. Diabetes. 2013; 62:1945–1956. [PubMed: 23349501]
36. Hetu PO, Riendeau D. Down-regulation of microsomal prostaglandin E2 synthase-1 in adipose tissue by high-fat feeding. Obesity (Silver Spring). 2007; 15:60–68. [PubMed: 17228032]
37. Claria J, Dalli J, Yacoubian S, Gao F, Serhan CN. Resolvin D1 and resolvin D2 govern local inflammatory tone in obese fat. J Immunol. 2012; 189:2597–2605. [PubMed: 22844113]
38. Lieb DC, Brotman JJ, Hatcher MA, Aye MS, Cole BK, Haynes BA, et al. Adipose tissue 12/15 lipoxygenase pathway in human obesity and diabetes. J Clin Endocrinol Metab. 2014; 99:E1713–E1720. [PubMed: 24955608]

What is already known about this subject?

Obesity is correlated with deregulated profiles of lipid mediators in adipose tissues.

Most studies only studied single or limited number of lipid mediators.

Previous studies focused on cyclooxygenase- and lipoxygenase-derived lipid mediators.

What does this study add?

We did a first lipidomics analysis of obesity in mice, which systematically analyzed >100 lipid mediators.

The results showed that P450-derived epoxy fatty acids, which were unappreciated in previous studies, were the most dramatically changed lipid mediators in obesity.

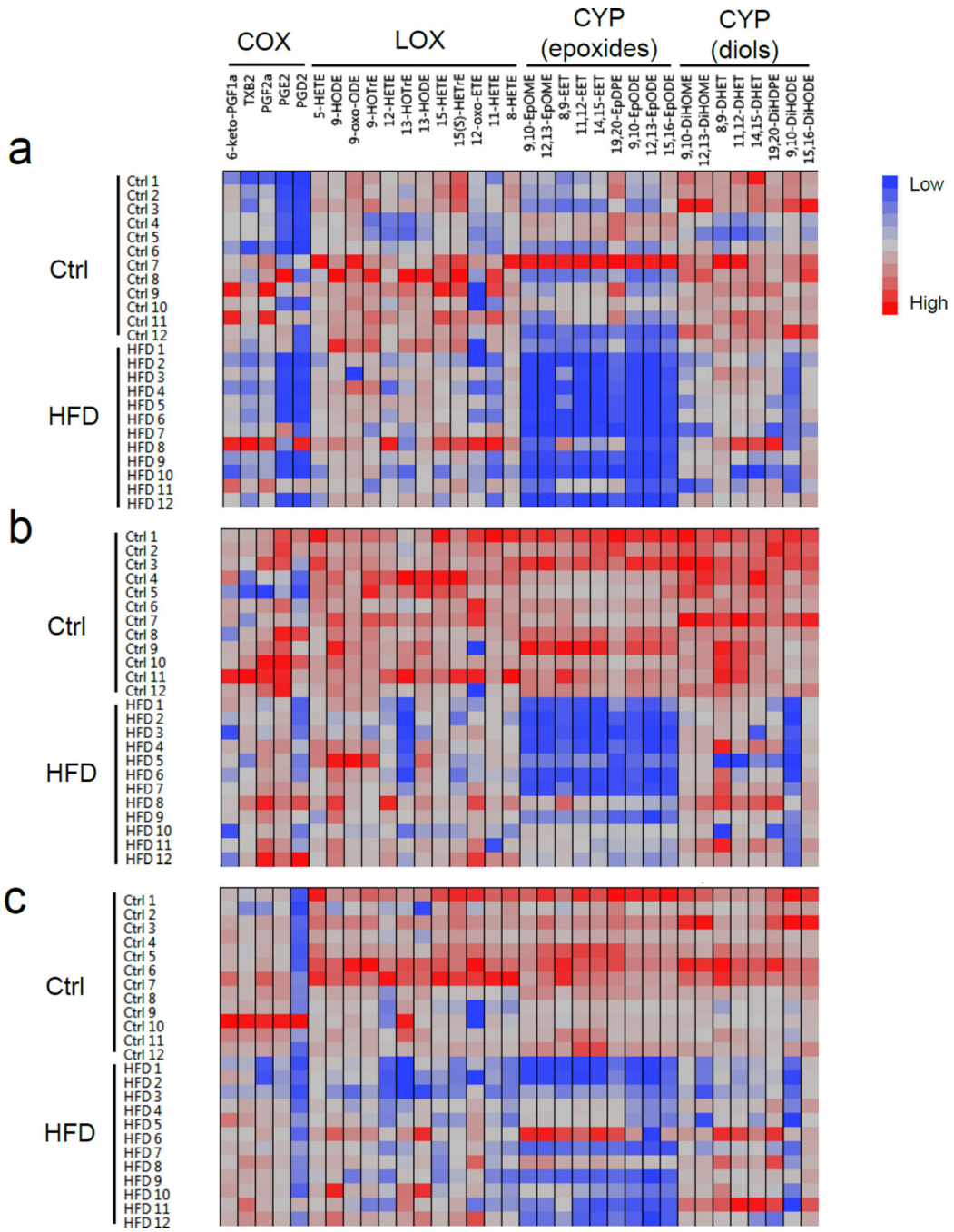

Figure 1.

Cell plot demonstarets that CYP-derived fatty acid epoxides are the most dramatically altered LMs in adipose tissues of HFD-fed mice. (***a***) inguinal adipose tissues. (***b***) gonadal adipose tissues. (***c***) interscapular adipose tissues. n = 12 mice per group.

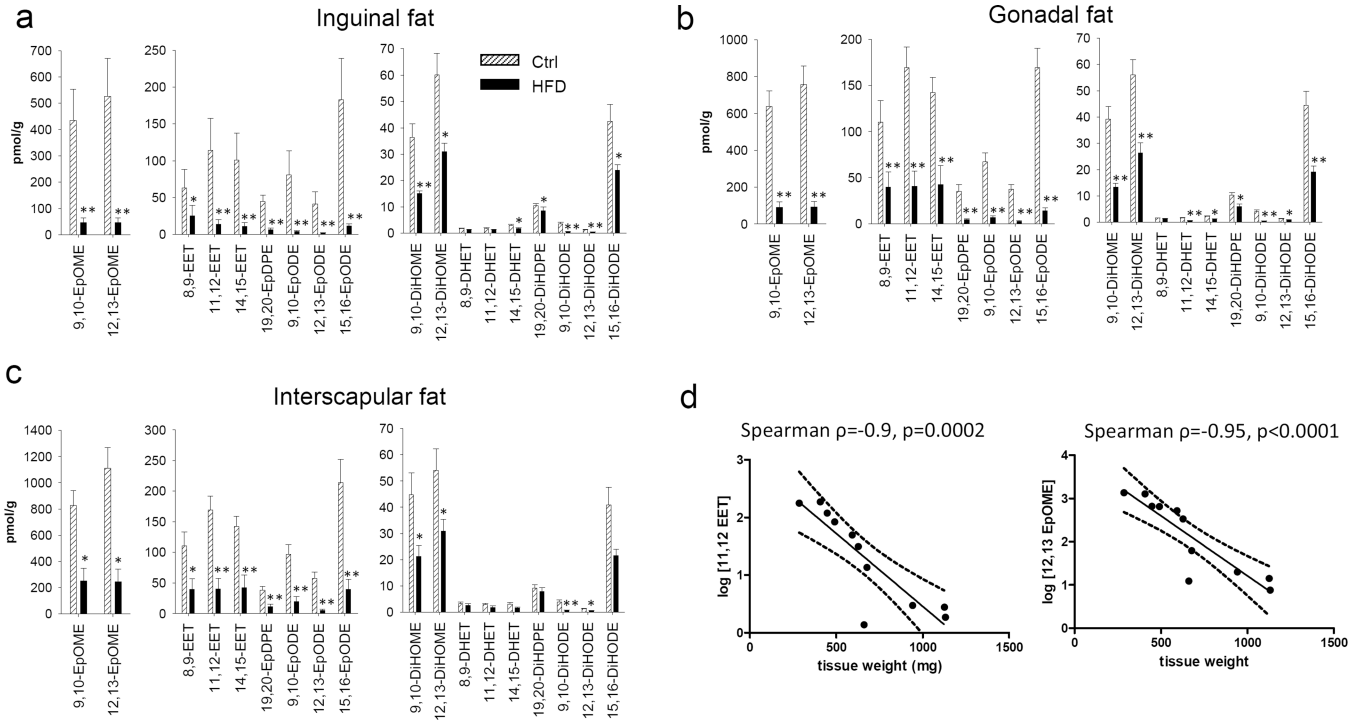

Figure 2.

Dietary feeding of HFD reduces levels of CYP-derived fatty acid epoxides and fatty acid diols in adipose tissues. (***a***) profiles of CYP-derived LMs in inguinal adipose tissues. (***b***) profiles of CYP-derived LMs in gonadal adipose tissues. (***c***) profiles of CYP-derived LMs in interscapular adipose tissues. (**d**) correlations of tissue concentration of fatty acid epoxides and tissue weight in gonadal adipose tissues. n = 12 mice per group, the results are mean ± SEM, * $P < 0.05$, ** $P \leq 0.001$.

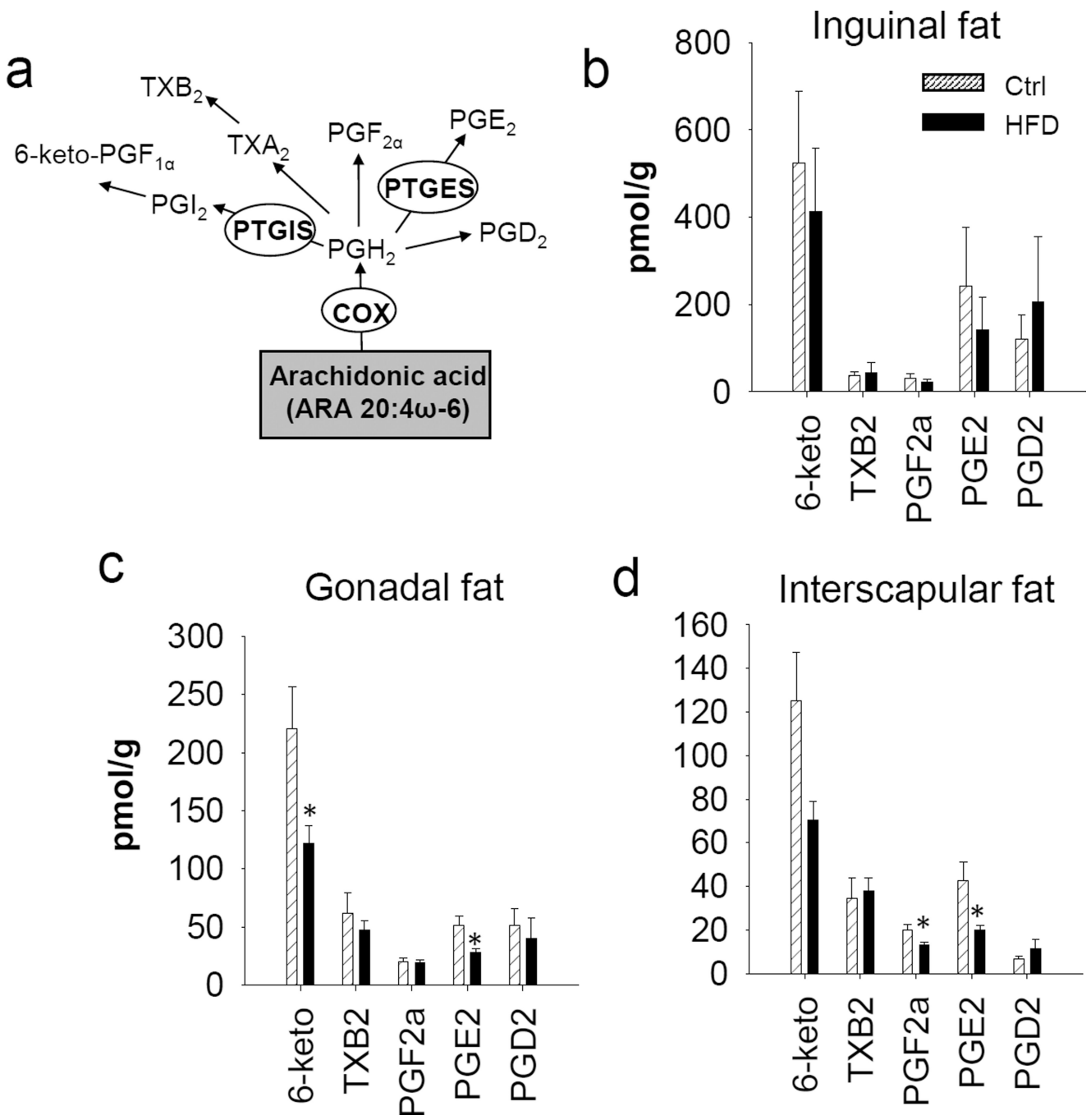

Figure 3.

Dietary feeding of HFD modulates COX-derived LMs in adipose tissues. (***a***) a simplified sheme of COX-2 pathway. Abbreviations: COX: cycloxygenase, PTGIS: prostacyclin synthase or PGI_2 synthase, PTGES: prostaglandin E synthase, see abbreviations of LMs in supplemental inforamtion Table S2. (***b***) profiles of COX-derived LMs in inguinal adipose tissues. (***c***) profiles of COX-derived LMs in gonadal adipose tissues. (***d***) profiles of COX-derived LMs in interscapular adipose tissues. n = 12 mice per group, the results are mean ± SEM, * $P < 0.05$.

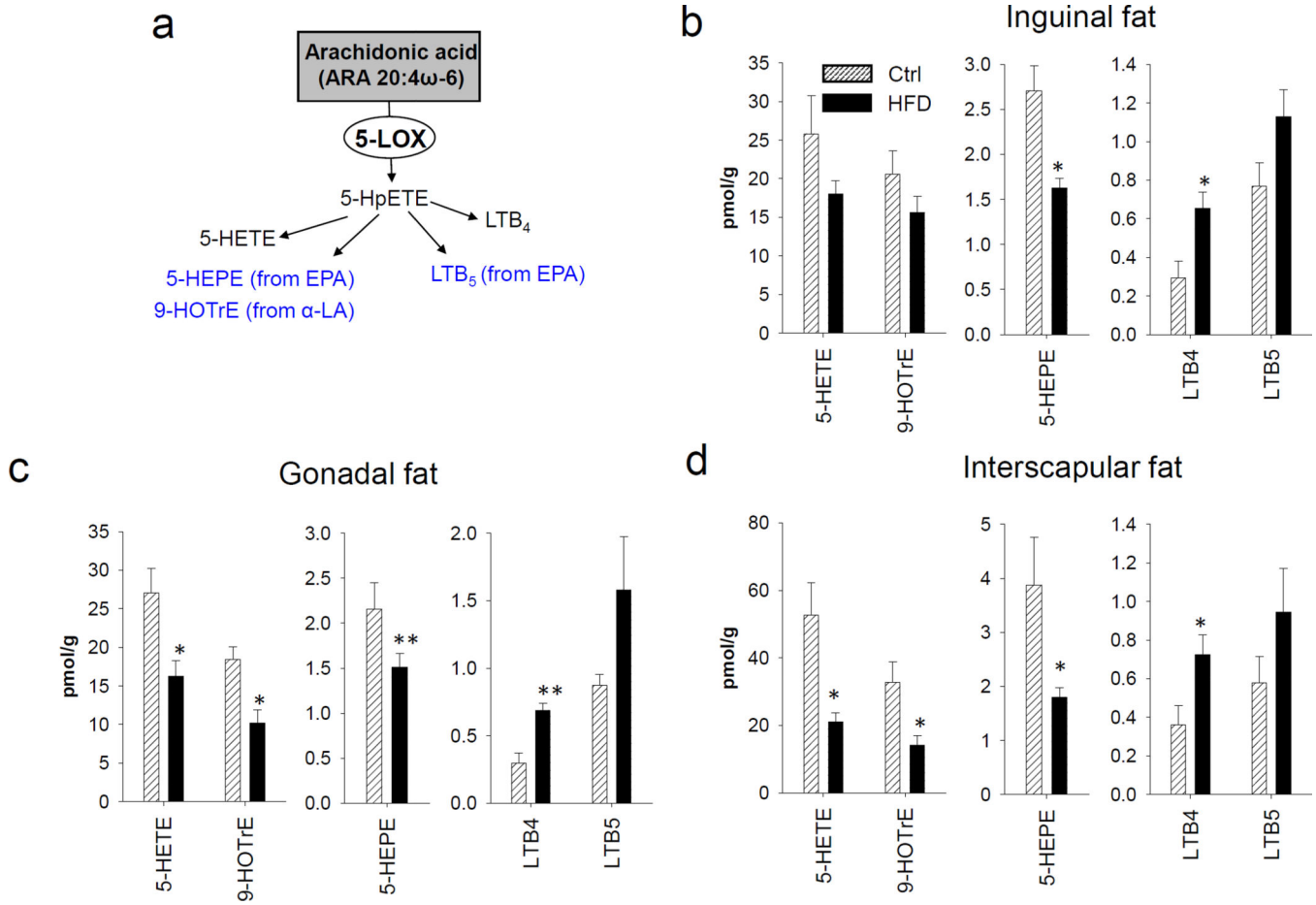

Figure 4.

Dietary feeding of HFD modulates 5-LOX-derived LMs in adipose tissues. (***a***) a simplified sheme of 5-LOX pathway. (***b***) profiles of 5-LOX-derived LMs in inguinal adipose tissues. (***c***) profiles of 5-LOX-derived LMs in gonadal adipose tissues. (***d***) profiles of 5-LOX-derived LMs in interscapular adipose tissues. n = 12 mice per group, the results are mean ± SEM, * $P < 0.05$, ** $P \leq 0.001$.

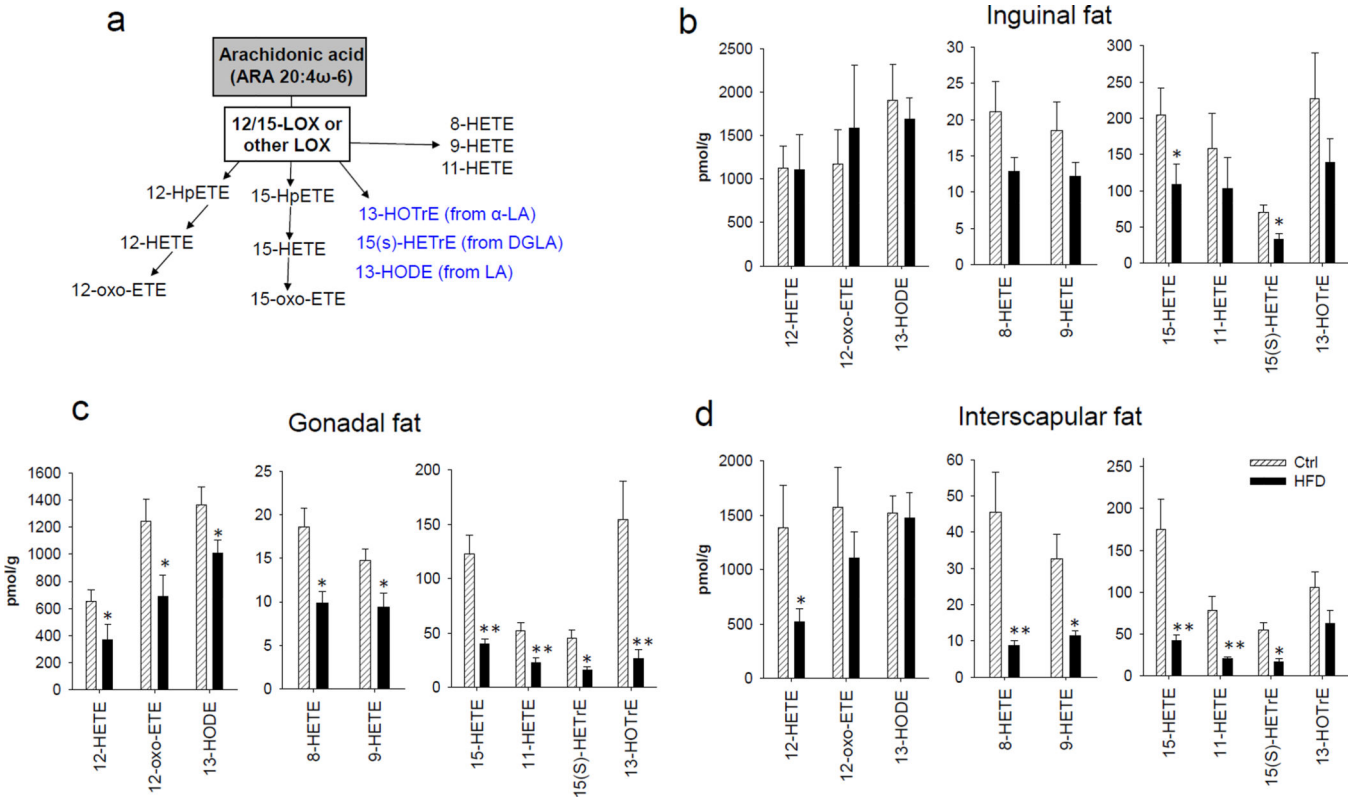

Figure 5.

Dietary feeding of HFD modulates 12/15-LOX-derived LMs in adipose tissues. (***a***) a simplified sheme of 12/15-LOX pathway. (***b***) profiles of 12/15-LOX-derived LMs in inguinal adipose tissues. (***c***) profiles of 12/15-LOX-derived LMs in gonadal adipose tissues. (***d***) profiles of 12/15-LOX-derived LMs in interscapular adipose tissues. n = 12 mice per group, the results are mean ± SEM, * $P < 0.05$, ** $P \leq 0.001$.

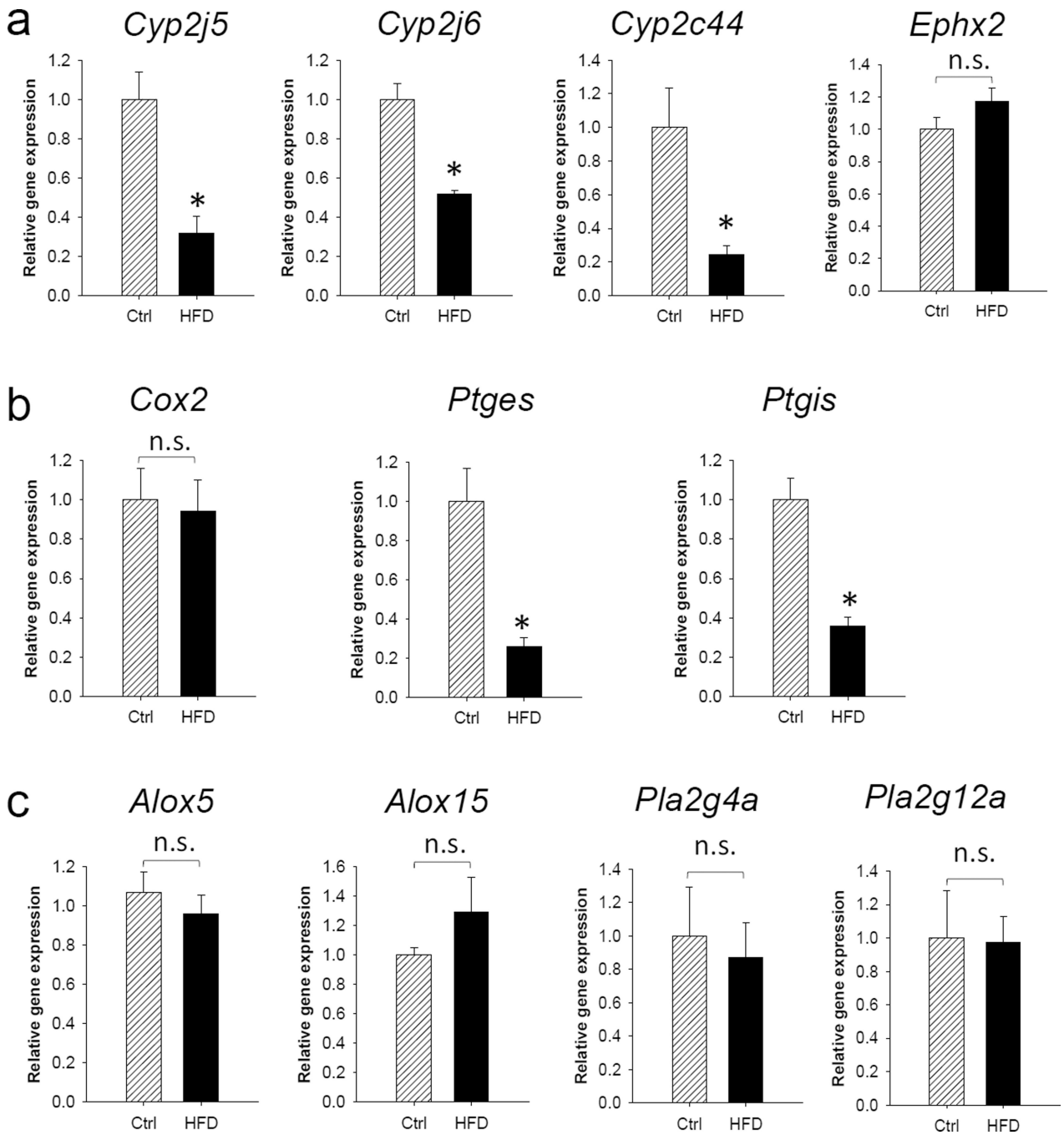

Figure 6.

Effect of HFD on gene expresions of PUFA metabolizing enzymes in gonadal adipose tissues. (***a***) gene expressions of enzymes involved in CYP pathway. (***b***) gene expressions of enzymes in COX pathway. (***c***) gene expressions of enzymes in LOX pathway, as well as phospholipase A_2 (PLA_2). n = 4–6 per group, the results are mean ± SEM, * $P < 0.05$, n.s. not significant.